Modal conversion with artificial materials for photonic-crystal waveguides

Philippe Lalanne, Anne Talneau

Modal conversion with artificial materials for photonic-crystal waveguides

Ph. Lalanne

Laboratoire Charles Fabry de l'Institut d'Optique, Centre National de la Recherche Scientifique, 91 403 Orsay Cedex, France
Philippe.lalanne@iota.u-psud.fr

A. Talneau

Laboratoire de Photonique et de Nanostructures, Centre National de la Recherche Scientifique, Route de Nozay, 91460 Marcoussis, France

Abstract: We study adiabatic mode transformations in photonic-crystal integrated circuits composed of a triangular lattice of holes etched into a planar waveguide. The taper relies on the manufacture of holes with progressively-varying dimensions. The variation synthesizes an artificial material with a gradient effective index. Calculations performed with a three-dimensional exact electromagnetic theory yield high transmission over a wide frequency range. To evidence the practical interest of the approach, a mode transformer with a length as small as $\lambda/2$ is shown to provide a spectral-averaged transmission efficiency of 92% for tapering between a ridge waveguide and a photonic crystal waveguide with a one-row defect.
©2002 Optical Society of America

OCIS codes: (130.3120) Integrated optics devices; (250.5300) Photonic integrated circuits

---

References and links

1. T. F. Krauss, R. M. De La Rue and S. Brand, "Two-dimensional photonic bandgap structures operating at near-infrared wavelengths," Nature **383**, 699-702 (1996).
2. D. Marcuse, *Light Transmission Optics* (Van Nostrand Reinhold, New York, 1972).
3. Y. Xu, R. K. Lee and A. Yariv, "Adiabatic coupling between conventional dielectric waveguides and waveguides with discrete translational symmetry," Opt. Lett. **25**, 755-757 (2000)
4. M. Palamaru and Ph. Lalanne, "Photonic crystal waveguides: out-of-plane losses and adiabatic modal conversion," Appl. Phys. Lett. **78**, 1466-69 (2001).
5. A. Mekis and J.D. Joannopoulos, "Tapered couplers for efficient interfacing between dielectric and photonic crystal waveguides," J. Lightwave Technol.**19**, 861-865 (2001).
6. T.D. Happ, M. Kamp and A. Forchel, "Photonic crystal tapers for ultracompact mode conversion," Opt. Lett. **26**, 1102-04 (2001).
7. Z. Weissman and A. Hardy, "2-D mode tapering via tapered channel waveguide segmentation," Electron. Lett. **28**, 1514-1516 (1992).
8. E. Silberstein, Ph. Lalanne, J.P. Hugonin and Q. Cao, "On the use of grating theory in integrated optics," J. Opt. Soc. Am. A. **18**, 2865 (2001).
9. N.P.K. Cotter, T.W. Preist, and J.R. Sambles, "Scattering-matrix approach to multilayer diffraction," J. Opt. Soc. Am. A **12**, 1097 (1995).
10. J.P Bérenger, "A perfectly matched layer for the absorption of electromagnetic waves," J. Computational. Physics, **114**, 185-200 (1994).
11. C.J.M. Smith, H. Benisty, S. Olivier, M. Rattier, C. Weisbuch, T.F. Krauss, R.M. De La Rue, R. Houdré and U. Oesterle, "Low-loss channel waveguides with two-dimensional photonic crystal boundaries," Appl. Phys. Lett. **77**, 2813-15 (2000).
12. Ph. Lalanne, "Electromagnetic analysis of photonic crystal waveguides operating above the light cone," to be published in IEEE Journal of Quantum Electronics.

---

1. Introduction

Photonic crystals (PC) are artificial optical materials with a strong periodic modulation that offers the possibility of controlling and manipulating light by opening a photonic band gap within a given range of frequencies. The creation of line defects in PC produces waveguide

modes within the photonic band gap. These modes are different from those of conventional waveguides that use total internal reflection and are expected to lead to compact photonic integrated circuits [1]. Because of the challenge to fabricate three-dimensional (3D) PC with submicronic feature sizes, much efforts are devoted to the fabrication of two-dimensional (2D) PC etched into planar waveguides. Like for conventional waveguides, transformation of modal properties through tapering is of significant practical interest. Mode-size transformation permits independent optimization of the mode profile for effective input and output coupling and for efficient performance of devices. Whereas adiabatic mode transformers are easily implemented for classical dielectric waveguides [2], the problem is radically different for PC waveguides [3-6]. In this work, we propose a general technique for tapering into PC waveguides. At the same time, we also provide a solution for tapering between PC waveguides and classical ridge waveguides, a crucial point for implementation.

As an example of mode transformation, we consider the geometry shown in Fig. 1, where a W1 waveguide is tapered and changed into a W3 waveguide. By Wn, we denote the waveguide formed by removing n rows of air cylinders in the ΓK direction of a PC crystal formed by a triangular lattice of air holes etched into a planar waveguide. In a PC integrated circuit, the modal conversion between Wn and WN waveguides, N>n, is of great practical interest. For instance, a microlaser is more efficiently implemented in a WN waveguide whereas a Wn operation is preferable for implementing sharp turns. As illustrated in Fig. 1, the taper is formed by a series of etches whose feature dimensions vary progressively. The progressive adaptation requires the manufacture of holes with lateral dimensions smaller than those of the PC. Due to a spatial averaging effect at the subwavelength scale, the taper implements an artificial material with a gradient effective index and an adiabatic mode transformation is implemented through the progressive and slow variation. This approach that was first suggested in [4] is radically different from previous proposals [3, 5-6], that all rely on a progressive reduction of the defect dimension. Although its principle of operation shares common features with tapered segmented waveguide [7], it presents radically different perspectives. Because the periodicity constant is more than an order of magnitude smaller than that of segmented waveguides used for tapering in conventional low-index contrast waveguides, the subwavelength segments of the taper potentially support genuine nonleaky Bloch modes that result in a lossless operation. Moreover, the subwavelength scale results in radically different taper lengths offering the perspective of high compacity.

2. Numerical study

Figure 2 shows the situations we chose to test numerically the efficiency of tapers. Figure 2(a) corresponds to the tapered situation, where a ridge waveguide is tapered and changed into a 8-row-long W1 waveguide and then back into a ridge waveguide. The incoupling or outcoupling are performed in two steps. The ridge waveguide is first coupled into a W3 waveguide and then tapered into a W1 waveguide. Figure 2(b) corresponds to the non-tapered situation. A ridge waveguide is coupled directly into a 18-row-long W3 waveguide and then back into a ridge waveguide. It will be used as a reference. For the computation, we assume that the PC crystal is composed of a triangular lattice of air holes with a fill factor (ratio of holes to total area) of 33%. This lattice possesses a large gap for TE-like modes. The holes are assumed to have straight side walls (perfect cylinders) and to have a finite depth h = 900 nm. In practice, the tiny holes required for manufacturing the taper are likely to have a smaller depth than the larger PC holes. The holes are etched through a planar waveguide composed of a GaAs (refractive index 3.5) 250-nm wide core with claddings with refractive indices 3.4 for the cover and 3.0 for the substrate. The cover thickness is 330 nm and the lattice parameter *a* is 220 nm, corresponding to a mid-gap wavelength of approximately 850 nm. The ridge lateral size is 3.46*a* and is also etched 900 nm-deep. Although an adiabatic transformation requires the manufacture of a series of holes with progressively-varing sizes, as shown in Fig. 2, we
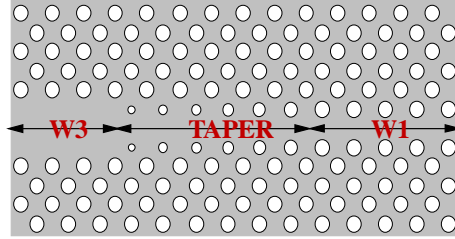
Fig. 1. Tapering with artificial materials between two different PC waveguides. Gray zones correspond to a high refractive-index material. The specific case of a W1-W3 mode conversion is illustrated for a triangular lattice of air holes.

consider a very short taper composed of only two holes in order to lower the computational loads. The smaller hole, H2, has a fillfactor of $\approx 4\%$ and the larger one, H1, has a fillfactor of $\approx 15\%$. The lower ridge is assumed to be illuminated by the fundamental TE_{00} mode with a unit intensity. For the tapered situation, R_1 and T_1 denote the modal reflection and transmission, respectively. R_2 and T_2 denote the related quantities for the non-tapered case.
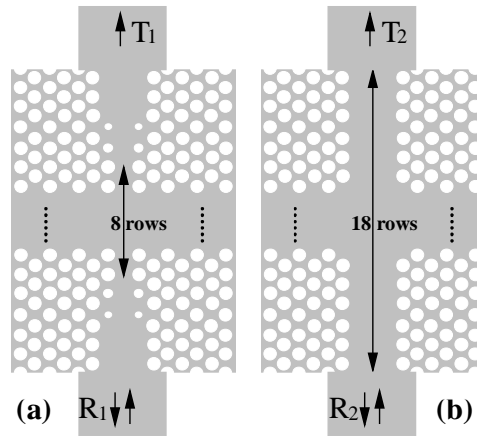

Fig. 2. Geometries considered for testing the taper principle. The lower ridge waveguides are assumed to be illuminated by the fundamental TE_{00} mode with a unit intensity. R_i and T_i denote the reflected and the transmitted intensities, respectively. (a) situation with tapers. To lower computational loads, only two different holes H1 and H2 are considered for the gradual variation. (b) situation without taper used as a reference. For both situations, the total length of the PC circuit is 18a.

The 3D computation is performed with the frequency-domain modal method described in [8]. In brief, the method relies on Fourier expansions for all the electromagnetic fields quantities and for the permittivity in the transverse plane (x, y). The real continuous profile along the z-direction is approximated by a stack of slices with piecewise-constant permittivities and in every slices, the modes and their propagation constants are computed exactly. By matching the boundary conditions at the slice interfaces, the S-matrix [9] relating the input and output field is computed recursively. Ten slices per PC row of length a were used to approximate the continuous profile. As shown in Fig. 3 where a typical cross section of one of the W1 slice is shown, Perfectly-Matched Layers [10] are used to delimit the computational domain. Thus out-of-plane scattering into the substrate and the air are accurately taken into account in the computation.

We first estimate the accuracy of the present approach by providing numerical test convergence. Because as many as three PC periods are taken into account on each side of the PC waveguide in the unit cell, see Fig. 2, the Fourier expansion along the y-direction is more demanding in computer resource than that along the x-direction. Figure 4 shows the

convergence performance of the method as a function of the truncation ranks for $\lambda = 0.8\ \mu m$. We denote by M_y and M_x the truncation rank along the y- and x- directions. By truncation rank M_α, we mean that a total of $2M_\alpha+1$ Fouriers harmonics are retained for the computation along the α-direction. Circles and squares represent T_1 data computed respectively as a function of M_y for $M_x = 5$, and as a function of M_x for $M_y = 27$. From Fig. 4, it is expected that the transmission T_1 can be predicted with an accuracy of ≈ 0.01 for $M_y > 25$ and $M_x > 5$. In this specific case with a mirror symmetry along the x-direction, the CPU time on a PC computer equipped with a Pentium IV processor (1.8 Ghz clock frequency) is ≈ 1.3 hour for $M_x = 5$ and $M_y = 35$. A Matlab sofware is used for the calculation without compiling the codes.
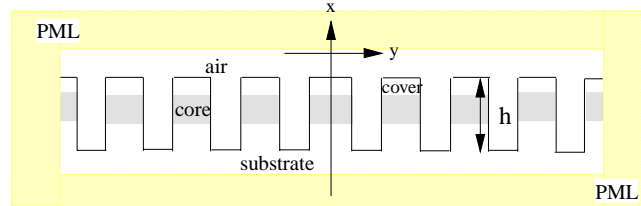

Fig. 3. Cross section of a slice used for the computation. Perfect Matched Layers are used at the boundary of the unit cell. The example corresponds to a slice of a W1 waveguide.
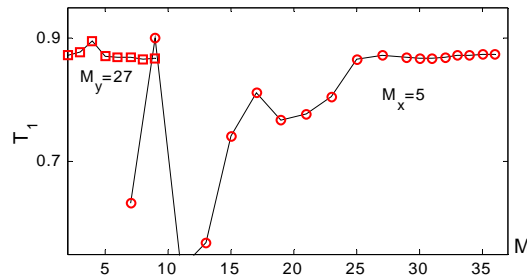

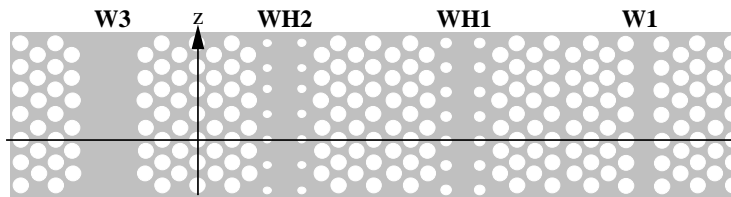Fig. 4. Convergence performance of the present method.

Fig. 5. Periodic waveguides associated to the taper segments. The horizontal line shows the z-plane location of the Bloch-mode profiles shown in Fig. 7.

3. Numerical results

For the following discussion, it is convenient to consider the periodic waveguides associated to the different taper segments. By WH1, we denote the periodic waveguides obtained by adding two rows of holes H1 on each side of a W3 waveguide, see Fig. 5. Similarly, WH2 is obtained by adding two rows of holes H2. In fact, an infinite set of periodic waveguides can be engineered by varying progressively the fillfactor of the added holes. The numerical transmission and reflection spectra for the diffraction problems of Fig. 2 are shown in Fig. 6. The horizontal axis covers the full band-gap spectral region, from $0.78\ \mu m$ to $0.98\ \mu m$. Circles and squares are obtained for the non-tapered and tapered situations, respectively. Except for $\lambda \approx 0.87\ \mu m$, the transmission T_2 is very high, the coupling between the ridge and the W3 waveguides is highly efficient. The low transmission at $\lambda \approx 0.87\ \mu m$ does not result from any

mode-mismatch problem. It is due to the hybridization of the fundamental W3-waveguide mode with a higher back-propagating order mode of W3. The hybridized mode acts as a lossy mirror. This phenomenon that corresponds to the opening of a mini-stop-band has been observed experimentally in Ref. [11].
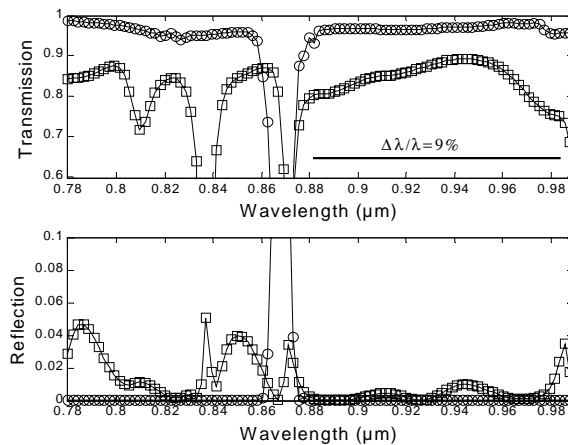

Fig. 6. Numerical results for the transmission (top) and reflection (bottom) spectra of the geometries shown in Fig. 2. The wavelength range covers the full band-gap spectral region. Circles : T_2, squares : T_1. The horizontal line indicate the spectral domain of interest.

The transmission spectra of the tapered situation is more complex. Two spectral regions can be identified. For low frequencies, the transmission spectrum is smooth, whereas several dips are observed for large frequencies. The dip for $\lambda \approx 0.87$ µm is due to the ministopband of the W3 waveguide. As shown by numerical results for the computation of the Bloch modes, WH-type waveguides have similar mini-stop-bands whose central frequencies shift to shorter wavelength as the hole fillfactor is increased. Although the tapered sections do not present any periodicity, we believe that the existence of mini-stop-band for WH-type waveguides reflects in the T_1 spectrum. For exemple, the dips at $\lambda \approx 0.84$ and 0.81 µm nearly coincide with the center wavelengths of the mini-stop-band of the WH2 and WH1 waveguides. If longer tapers with progressively varying holes dimensions were implemented, the existence of mini-stop-bands would prevent a good performance for $\lambda < 0.88$ µm. This is the reason why the following discussion is related to the spectral interval indicated by an horizontal line in Fig. 6. This interval with a relative spectral width $\Delta\lambda/\lambda$ of 9% is large enough for many applications.

Over this spectral region, the minimum and maximum values for T_1 are 80% and 90%. On average, the transmission T_1 is 85%. The amount of reflected light is rather weak, the maximum value for R_1 being 1% with an average value of 0.4%. Thus, approximately 15% of the light is scattered into the substrate and in the air. Two different mechanisms contribute to the loss. For the low-index-contrast waveguide considered in this work, the W1 and W3 waveguides are leaky. The attenuation of the W1 waveguide is ≈ 10 dB/100µm and that of the W3 waveguide is two order of magnitude smaller [12]. Thus $\approx 3\%$ of the light is lost by propagation in the 8-row-long W1 waveguide. The main channel for loss is the mode mismatch at the taper section. This mismatch mainly results in radiation into the claddings.

Considering that the diffraction problem results from a double coupling between a ridge and a W1 waveguide and neglecting the 3% loss due to the propagation along the 8-row-long W1 waveguide, two quantities of practical interest can be deduced from the transmission T_1 : the efficiency $(T_1)^{1/2}$ for a single coupling between a ridge and a W1 waveguide, and the tapering efficiency $(T_1/T_2)^{1/2}$ for a single coupling between W3 and W1 waveguides. On spectral average, these two quantities are 92% and 94%, respectively. These efficiencies correspond to good performance, especially if one considers that only two holes (taper length

$\approx 2a$) were considered to lower the computational loads. Moreover, the efficiency of 92% is comparable to that obtained in related works [3,6], for which it is worth emphasizing that the taper performance was estimated numerically with a 2D software that is not able to take into account out-of-plane radiation scattering, a crucial loss channel in this problem.
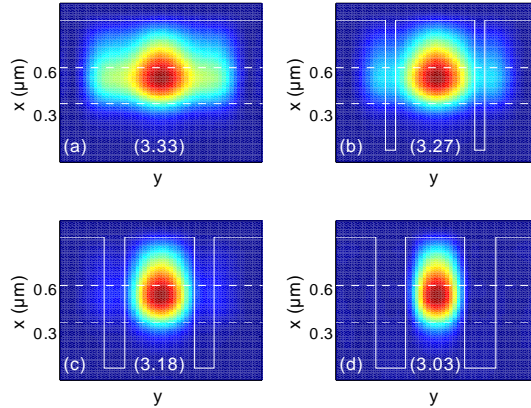

Fig. 7. Bloch-mode profiles for the different taper sections for $\lambda = 0.9$ µm. The effective indices (real parts) are given in parentheses. The horizontal dashed lines correspond to the stack interfaces cover/core/substrate. (a), (b), (c) and (d) correspond to the W3, WH1, WH2 and W1 waveguides. The profiles are obtained at longitudinal locations indicated by the horizontal solid lines in Fig. 5.

It is interesting to further consider the electromagnetic quantities that are involved into the tapering process. These quantities are clearly the fundamental TE_{00} mode supported by the ridge waveguides, and as shown in Ref. [4], the fundamental Bloch modes associated to the different sections of the taper. These sections are the W3, W1, WH1 and WH3 waveguides of Fig. 5. Figure 7 shows the different mode profiles (magnitude of the square of the x-component of the magnetic-field vector) for $\lambda = 0.9$ µm. The real part of the corresponding effective indices are given in parentheses. As shown by a comparison of the different profiles, the modes are progressively transformed. At the same time the effective indices vary monotonically from 3.04 for W1 to 3.33 for W3. The effective index of the ridge waveguide is 3.34. This monotonic variation confirms that the taper acts as a gradient-index thin film.

4. Conclusion

In this work, a new technique for tapering with subwavelength segments has been proposed and validated through 3D computational results. The approach, that exploits the analogy between subwavelength periodic structures and artificial homogeneous media, implements a gradient-effective-index structure through a progressive variation of the feature sizes. Because of the subwavelength periodicity, very short tapers can be implemented. The 3D computational results show that a taper length as short as of $\lambda/2$ (two PC periods) can achieve a 92% efficiency for coupling between a conventional ridge waveguide and a PC waveguides with a one-row defect. It should be emphasized that the concept used in this work for adiabatic transformation is general. The triangular lattice with holes may be replaced by other lattice and atom geometries and the approach can be easily generalized to engineered waveguide geometries with improved line defects.

Acknowledgments